Carbon Nanocages as Heavy Metal Ion Adsorbents

David M. Burke[a], Justin O'Byrne[a], Peter G. Fleming[a], Dipu Borah[a], Michael A. Morris[a,b] and Justin D. Holmes[a,b,*]

a) Materials and Supercritical Fluids Group, Department of Chemistry and Tyndall National Institute, University College Cork, Cork, Ireland.

b) Centre for Research on Adaptive Nanostructures and Nanodevices (CRANN), Trinity College Dublin, Dublin 2, Ireland

*To whom correspondence should be addressed Tel: +353 (0)21 4903608; Fax: +353 (0)21 4274097; Email: j.holmes@ucc.ie

Abstract

Heavy metal ion contamination in drinking water poses a major risk to human health, whilst contamination in wastewater streams can cause damage to the wider environment. In this study carbon nanocages, synthesised using a supercritical fluid deposition method, were examined as adsorbents of Pb^{2+} ions from aqueous solutions. Through careful selection of the catalyst and the carbon deposition temperature and pressure, high yields of nanocages with surface areas up to 1175 m^2 g^{-1} were synthesised. These high surface area materials were subsequently tested for their ability to absorb Pb^{2+} ions, as a function of pH, from simulated wastewater. The nanocages were found to be effective at removing the Pb^{2+} ions to levels of 11.1 mg g^{-1}, compared to 7.6 mg g^{-1} for commercially available activated carbon. The kinetics of metal ion adsorption by the nanocages and activated carbon could be

described by a pseudo-second-order kinetics model, with a rate coefficient (k_2) of 4.8×10^2 g mg^{-1} min^{-1}.

Keywords: carbon; nanocages; lead ions; adsorption; remediation

1 Introduction

Heavy metal ion contamination in waste and drinking water are harmful to human health and the wider environment. Heavy metal ions are listed as high priority contaminants by both the 2007 CERCLA Priority List of Hazardous Substances compiled by the US EPA (ATSDR, 2007) and the European Union Restriction of Hazardous Substances Directive (RoHS, 2003) [1, 2]. Directives have been enforced by both agencies restricting the use of these substances in manufacturing and also limiting the acceptable level of these contaminants in drinking water. Classification of hazardous substances takes into account a combination of factors including frequency, toxicity and potential for human exposure. The accumulation of heavy metal ions in the human body can lead to many debilitating effects, such as joint and muscle pains to digestive problems and learning difficulties [3-5]. Removal of metal ions from drinking water in wastewater treatment centres has become a major issue and several methods are generally used such as ion exchange [6, 7], electrochemical [8,9], membrane separation [10] and adsorption [11-13]. Adsorption is currently the cheapest and most effective means of removing metal ions from wastewater. The most commonly used materials are activated carbons [11, 14, 15], zeolites [13], clays [12] and biomaterials [16, 17]. Activated carbons can be produced from cheap carbon precursors by pyrolysis at high temperatures (generally 400-900 °C). Pyrolysis will burn off any biomass and other volatile contents of the material which in turn produces carbon structures with high surface areas, a high degree of porosity and the potential for abundant adsorption sites with pre- or post-

chemical or physical processing. Activated carbons for lead removal have been produced from diverse and abundant supplies of raw materials. High surface area carbon matrices have been produced from coconut shells [18, 19], cattle manure [20] and eucalyptus bark [21] to name just a few. Functional groups can be introduced onto the surface of activated carbons using oxidative chemical reagents. The activation of carbon surfaces can take place before pyrolysis by soaking or impregnating the raw materials (carbon precursors) with highly oxidising acids, bases or salts [22-24]. Babel *et al.* have shown that nitric acid is a more effective oxidising acid than sulphuric acid for treating granular activated carbon for Cr ion removal [22]. Physical activation can also be used by introducing steam and/or CO_2 into the pyrolysis process. Girgis *et al.* carried out a comprehensive study using peanut hulls, H_3PO_4, steam and KOH over a range of different impregnation compositions, temperatures and pyrolysis times [23]. Carbons with high surface areas and pore volumes, up to 1177 $m^2\ g^{-1}$ and 0.597 $cm^3\ g^{-1}$ respectively, were obtained by impregnating peanut hull with 85 % H_3PO_4 in a 1:1 weight ratio followed by pyrolysis at 500 °C for 3 hr. Consequently this sample also exhibited the highest adsorption capacity when tested for the removal of methylene blue. However, post processing with acids to introduce functional groups onto the surface of the pyrolysed products can often lead to a reduction in surface area, due to the collapse of the carbon structure due to oxidation [25]. This oxidative surface functionalisation process, while reducing the surface area, also causes pore widening which can result in a more kinetically favourable uptake of metal ions [26].

Carbon nanocages (CNCs) are hollow graphitic cages similar to fullerene structures, but can be multilayered and have irregular shapes unlike the traditional fullerene spheres, and are often produced as a by-product of carbon nanotube (CNT) growth [27,28]. CNTs themselves have shown excellent adsorption capacities and desorption is facile by simple acid washing

without compromising the structure of the CNTs [29]. The surface area of pristine CNTs, which is typically below 100 m^2 g^{-1}, can be increased to 830 m^2 g^{-1} through post processing by chemical activation or heat treatment [30-32]. Exfoliation of carbon layers and the introduction of defects in the carbon lattice by acid treatment contribute to the increasing surface area of CNTs. In this study, CNCs synthesised by the supercritical deposition of *p*-xylene over Co/Mo/MgO catalysts, using a method previously reported by Li *et al.* [33], were examined as adsorbents of lead ions (Pb^{2+}) from aqueous solutions. A comparative study was carried out with commercial activated carbon purchased from Fluka Chemika to gauge the performance and viability of CNCs.

2 Experimental

2.1 Synthesis and Characterisation of CNCs

CNCs were synthesised using a supercritical fluid deposition method previously reported by Li *et al* [33]. Briefly 0.5 g of Co/Mo/MgO catalyst was placed in a reaction cell which was heated to 700 °C at a rate of 5 °C min^{-1} under a flow of argon (200 ml min^{-1}). The catalyst was reduced in 10 % H_2/Ar for 30 min at a flow rate of 200 ml min^{-1}. 3 ml of *p*-xylene was placed in the front part of a delivery cell, separated by a piston, in a water bath at 40 °C. The front part of the cell was then charged with CO_2 up to the desired reaction pressure using an ISCO pump. The contents of the supercritical fluid cell were flowed over the catalyst material in the reaction cell and CO_2 was applied to the back of the piston in the delivery cell to maintain a constant pressure throughout the course of the reaction. After the reaction was complete, the cell was depressurised and allowed to cool to room temperature under a flow of argon (200 ml min^{-1}). The catalyst material was removed by stirring in 3 M HNO_3 for 4 hr,

then filtered and washed with deionised water until the acidity of the filtrate was at pH 6 ,and finally dried at 60 °C in an oven for 24 hr.

2.1 Characterisation

Transmission electron microscopy (TEM) of the CNCs were performed on a JEOL 2000FX microscope operating at 200 kV, and high-resolution TEM images were obtained on a JEM 2010 microscope operating at 200 kV. Samples were prepared for TEM analysis by dispersing the material in ethanol and dropping onto copper grids. Scanning electron microscopy (SEM) analysis of CNCs and commercial activated carbons, to identify their morphologies, were conducted on a JEOL 5510 SEM. The powder samples were placed on carbon tape and then adhered to a brass stub. The surface areas of the carbon sorbent materials were measured using a Micromeritics Gemini 2375 volumetric analyser. Each sample was degassed for 5 hr at 200 °C prior to measurement. The surface area was calculated using the Brauner Emmett Teller (BET) method based on the adsorption data in the relative pressure (P/P_0) region of 0.01-0.99. Single-point pore volume was evaluated by converting the amount adsorbed at P/P_0 = 0.99 to the volume of liquid nitrogen [34]. Characterisation of CNCs by X-ray photoelectron spectroscopy (XPS) was carried out on a VSW Atomtech system using a non-monochromated Al X-ray source. Survey spectra were an average of 5 scans captured at a pass energy of 100 eV, a step size of 0.7 eV and a dwell time of 0.1 s. Level spectra were an average of 30 scans captured at a pass energy of 20 eV, a step size of 0.2 eV and a dwell time of 0.1 s. The final concentration of Pb ions in solution after adsorption was measured on a Perkin-Elmer 2280 Atomic Adsorption Spectrophotometer (AAS). The solutions were aspirated and mixed with acetylene before being ignited in a flame. A single element hollow cathode lamp was used which adsorbs light at the most dominant characteristic wavelength, which was at 217.0 nm for Pb.

2.3 Determination of Zero Point Charge.

The point of zero charge (pH_{pzc}) of CNCs and commercially available activated carbon (AC) was measured using a batch equilibrium technique. 50 ml of 0.1 M $Na(NO_3)$, used as an inert/background electrolyte, was placed in a beaker and the initial pH of the solution was adjusted using 0.01 M NaOH and/or 0.01 M HNO_3. 50 mg of the adsorbent material was then added to the solution and stirred for 24 hr to allow the pH of the suspension to equilibrate. The mixture was filtered and the final pH of the solution was measured using a pH meter. Experiments were completed for initial pH values ranging between 3-11, at an interval of approximately 1.0 pH unit. This equilibrium time allows for a plot of $pH_{initial}$ vs pH_{final} and the plateau that emerges can be taken as the pH_{pzc} of the material.

2.4 Dispersability of Sorbent Materials in Aqueous Media

The dispersability of CNCs and activated carbon was observed by mixing 15 mg of sorbent in 15 ml of deionised H_2O (concentration of 1 g dm^{-3}) and sonicated for 20 min to form a homogeneous suspension. The suspensions were then left to stand and pictures were captured on a Samsung S630 digital camera at regular intervals to observe the time taken for the materials to agglomerate.

2.5 Flowability of Aqueous Media through Sorbent Materials

A comparative test was used to examine the ease of flow of an aqueous solution through a fixed bed of CNCs and activated carbon. The system was set up by packing a fixed mass of cotton wool into a glass pipette and 20 mg of sorbent materials placed on top to form the sorbent bed. Another fixed mass of cotton wool was then packed above the sorbent bed to prevent dispersion of the sorbent powders into the aqueous media. An aqueous solution of

methyl blue (used as a colorant) was then flowed through the system and timed from when the aqueous solution was added to the system to the instant the first drop exited the system.

2.6 Adsorption of Pb ions from Aqueous Solutions

CNCs were tested as an adsorbent material for heavy metal ions from aqueous solutions using a batch adsorption technique. Parallel batch adsorption tests were carried out using activated carbon (AC) purchased from Fluka Chemika to compare with the CNCs. A 1000 mg dm^{-3} stock solution of Pb^{2+} were made by dissolving $Pb(NO_3)_2$ in deionised water.

2.6.1 Varying the pH

25 mg dm^{-3} stock solutions of Pb^{2+} ions were prepared by diluting 1000 mg dm^{-3} stock solutions described above in deionised water and adjusting the pH of the solution using 0.01 M NaOH or 0.01 M HNO_3. Typically 20 ml of a 25 mg dm^{-3} of the Pb^{2+} ion solution and 10 mg of the adsorbent material were placed in a beaker and stirred for 4 hr to allow for adsorption equilibrium in accordance with previous publications [15]. The final concentration of metal ions in solution that were not adsorbed by materials was measured on an AAS and the adsorption efficiency was calculated using equation (1) below:

$$q_e = (C_0 - C_e) \times V/m \quad (1)$$

where q_e is the metal uptake on the adsorbent under equilibrium conditions (mg g^{-1}); C_0 and C_e are the initial and final concentrations of metal ions in solution (mg dm^{-3}); V is the volume of the metal ion solution (dm) and m is the mass of adsorbent used.

2.6.2 Effect of Agitation Time, Initial Concentration of Metal Ions

The batch adsorption method was used to study the uptake of metal ions on the carbon adsorbents. Stock solutions of Pb^{2+} ions (25 mg dm^{-3}) were made up in buffered solutions at pH 5 (50 mM acetate buffer). 20 ml of each solution was agitated with 10 mg of adsorbent for a 4 hr before filtering and measuring of the final metal ion concentration.

3 Results and Discussion

3.1 Synthesis and Characterisation of Adsorbent Materials

Figure 1(a) shows a TEM image of an unpurified CNC sample, showing that carbon encapsulation takes place around the Co/Mo/MgO catalyst particles. The lattice ordering of MgO is visible with graphitic carbon layers forming around the crystal particles. The Co and Mo catalyst particles are not visible and it can be assumed they are dispersed across the surface of the MgO particles. The diameters of the CNCs, ranging from 20-50 nm, indicate that carbon forms around the entire catalyst particle as opposed to a single metal nanoparticle, indicating that the MgO support has a pivotal role to play in the formation of CNCs [35]. Li *et al.* have suggested that MgO can react with CO_2 to form $MgCO_3$ but is unstable and reverts back to MgO and CO_2 above 660 °C at 0.1 MPa [33]. This would explain the large diameter of the cages and also the irregularity in the distribution of CNC diameter and shape as the composition of MgO and $MgCO_3$ is in a state of flux during the course of the reaction. In our study the reaction conditions of 10.34 MPa and 700 °C and the unstable nature of the $MgCO_3$ particles under these conditions would account for the irregular CNC diameter distributions. Mild acid treatment in 3 M HNO_3 efficiently removes the catalyst to leave the hollow carbon structures as shown in figure 1(b). The morphologies of CNC and activated carbon (AC) samples is shown in the SEM images in figure 2. Both the CNC and AC samples have highly porous yet contrasting morphologies. The CNC sample displays agglomeration of individual

nanocages, with an abundance of interstitial space, whereas the AC exhibits larger particles with narrower interstitial spaces; as confirmed by nitrogen physisorption measurements.

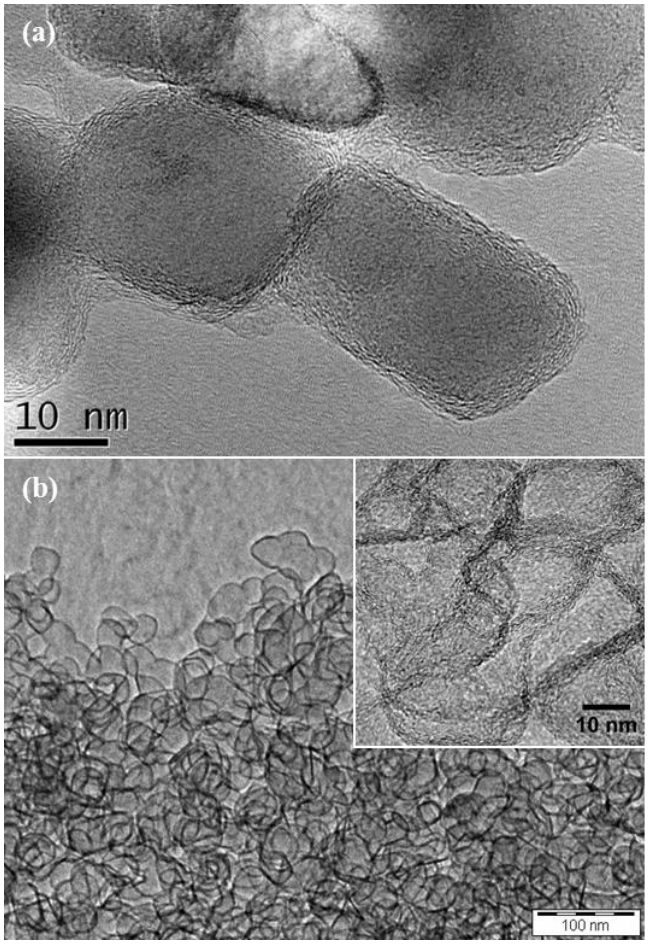

Figure 1. TEM images of (a) unpurified CNCs where the catalyst is still visible (inset shows the crystalline MgO core) and (b) purified CNCs where the catalyst has been removed to leave hollow cage structures (inset TEM image of purified CNCs).

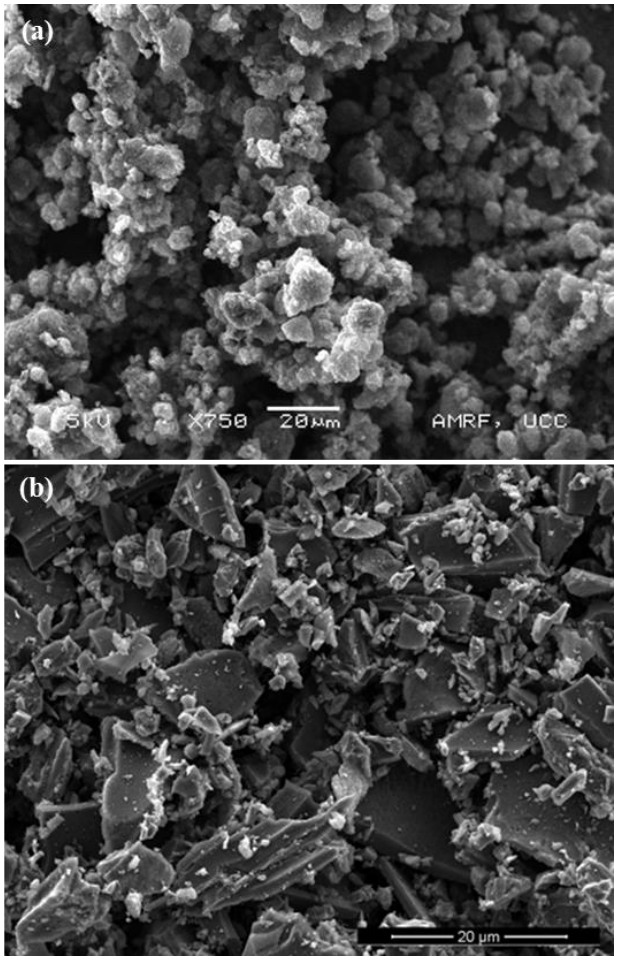

Figure 2. SEM images showing the morphologies and pore structures of (a) purified CNC1 and (b) AC.

Table 1. Physical characteristics of the CNCs and carbonic adsorbents including nitrogen physisorption data and pH_{pzc}.

Sample	**T**	**P**	**Yield (carbon/ wt. catalyst)**	**pH_{pzc}**	**S_{BET}**	**Total Pore Volume V_{tot}**	**Average Pore Diameter d_P**	**% O**
	°C	MPa	%		$m^2\ g^{-1}$	$cm^3\ g^{-1}$	nm	
CNC	700	10.34	13.5	7.02	1176	7.0	24	5.9
CNCa	750	10.34	17.7		765	5.9	31	
CNCb	700	8.23	12.6		1286	6.1	19	
Activated Carbon			n/a	7.49	526.90	0.3	4	4.1

The CNCs and ACs both have porous morphologies. Nitrogen physisorption data for all of the CNC samples synthesised in this study and the commercial AC are given in table 1. CNCs were produced under the following conditions CNC (T = 700 °C, P_{CO2} = 10.34 MPa), CNCa (T = 750 °C, P_{CO2} = 10.34 MPa) and CNCb (T = 750 °C, P_{CO2} = 8.27 MPa. CNCs generated at 700 °C had the highest surface areas (mean S_{BET} = 1176 m^2 g^{-1}). At growth temperatures above 750 °C, the mean surface area of the product decreased (S_{BET} = 765 m^2 g^{-1}) due the greater feed of carbon resulting in thicker CNC shells. Table 1 shows the effect of altering the reaction pressure from 10.34 to 8.27 MPa which resulted in a slight increase in S_{BET} but also a significant reduction in the carbon yield, from 13.5 to 12.6 % respectively, and also a narrowing of the pore diameter from 24 to 19 nm.

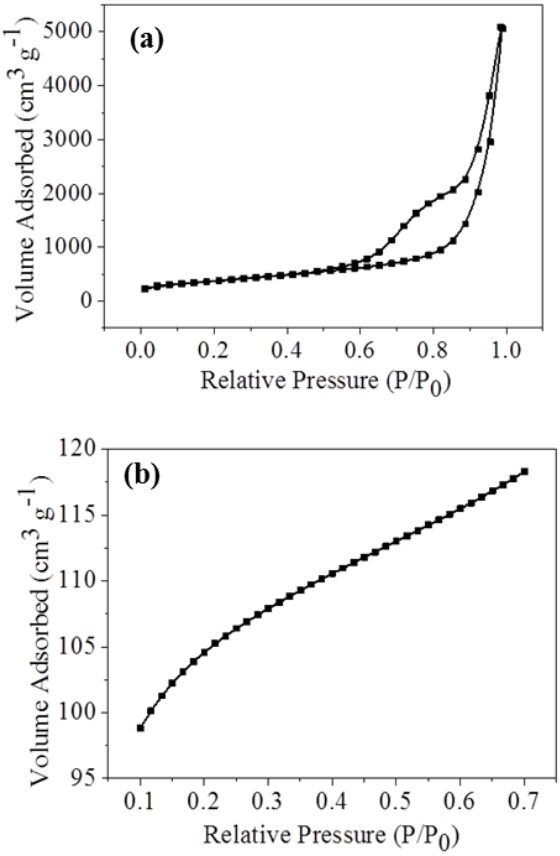

Figure 3. Nitrogen physisorption data for (a) purified CNCs grown at T = 700 °C, P = 10.34 MPa for a reaction time of 1 hr and (b) AC.

Figure 3 shows nitrogen physisorption curves for CNCs produced at 700 °C and 10.34 MPa. Type IV hysteresis was observed in the physisorption data for all of the CNC samples examined, indicating mesoporous character [34]. A plot of pore diameter generally gives a bi-modal plot for CNCs indicating two distinct regions of mesoporous adsorption: (i) the hollow cavity of the CNCs and (ii) the interstitial porous regions between the agglomerated CNCs. Activated carbon had a much lower surface area (S_{BET} = 527 m^2 g^{-1}), compared to the CNC sample (prepared at T = 700 °C and P = 10.34 MPa) and displayed a type I isotherm curve, indicative of a microporous structure.

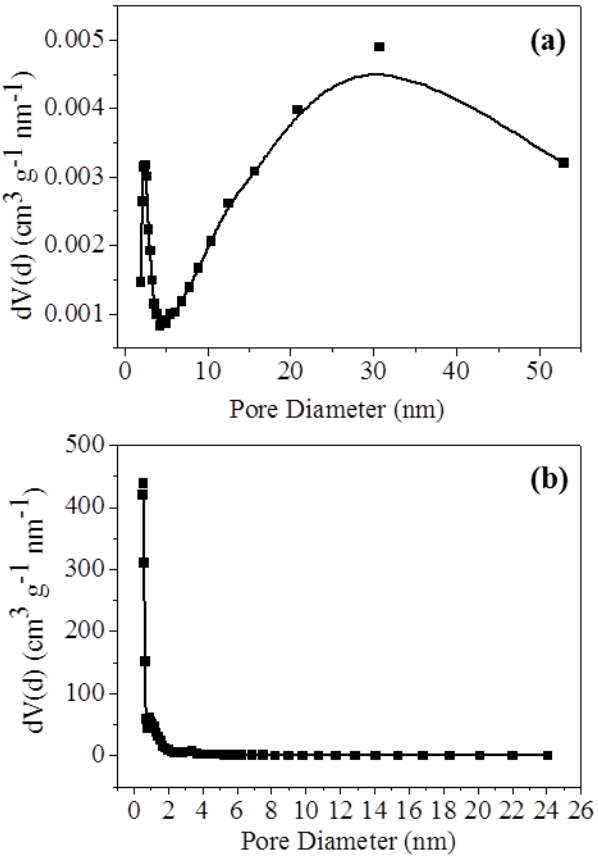

Figure 4. Nitrogen physisorption data showing pore size distribution for samples of (a) purified CNCs, grown at T = 700 °C, P = 10.34 MPa for a reaction time of 1 hr and (b) AC.

An average pore diameter of 24 nm was also recorded for the CNCs, although a study of pore size distribution (figure 4(a)) showed a bimodal plot with mesopores in the 2-6 nm range and also a second distribution in the 5-55 nm range. Pore size distribution analysis of the AC (figure 4(b)) showed almost 100 % microporosity with a mean pore diameter of 4 nm (table 1) recorded by N_2 physisorption measurements.

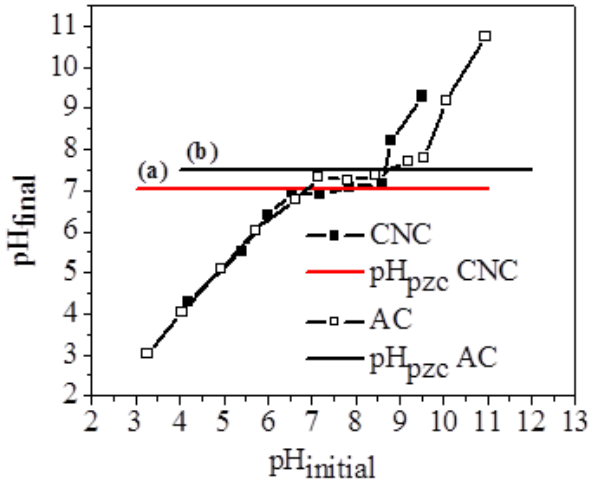

Figure 5. Graph showing pH_{pzc} data for purified CNCs and AC using a plot of $pH_{initial}$ vs pH_{final} , pH_{pzc} is indicated on the graph for (a) CNCs and (b) AC. Sorbent loading, 50 mg; background electrolyte, 0.1 M $NaNO_3$; equilibration time, 24 hr.

The pH_{pzc} of CNCs and activated carbon were both close to neutral, *i.e.* 7.02 and 7.49 respectively, as shown in figure 5. The pH_{pzc} value is dependent on the acid-base relationship of the material; the pH_{pzc} is the solution pH where there will be a neutral charge on oxygenated sites which result in a net neutral charge on the surface of the absorbent. The lower pH_{pzc} value for the CNCs suggests that the material will be a slightly more effective adsorbent at lower pH values, due to the higher density of acid sites compared to AC.

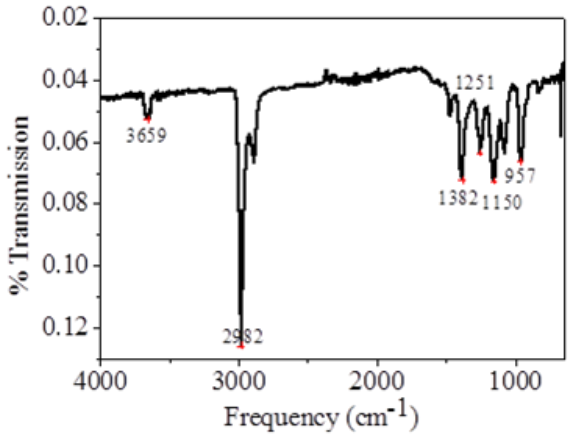

Figure 6. FTIR of purified CNCs synthesised at T = 700 °C, P = 10.34 MPa for a reaction time of 1 hr.

Li *et al.* have previously shown that C=O and C-O oxygenated surface groups exist on the surface of CNCs [33]. The mean composition of the CNCs obtained from XPS was found to be 94.1 % carbon and 5.9 % oxygen, whereas the mean composition of the AC samples was 95.9 % carbon and 4.1 % oxygen. Figure 6 shows an FTIR spectrum of the CNCs which displays a sharp peak at 3659 cm^{-1}, associated with a hydroxyl group (-OH), and also vibrations at 1382 cm^{-1} (C-O-H) and 1251 cm^{-1} (C-O) associated with the carboxylic acid groups on the surface of the adsorbent.

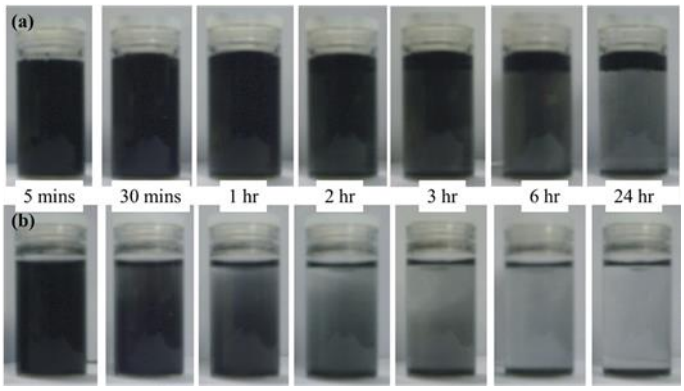

Figure 7. Images of (a) CNC and (b) activated carbon dispersed in aqueous solution at a loading of 1 g dm^{-3} and the effect of time on settling.

Figure 7 shows the effect of the dispersing CNCs and activated carbon samples in aqueous media, in which both sorbent materials readily disperse. This is due to the oxidation of the carbon surface, introducing a profusion of functional groups across the surface of the materials, which are hydrophilic in nature allowing homogeneous dispersion of the sorbent materials [36]. Figure 7 also shows that the CNCs remain in suspension for a greater amount of time (up to 24 hr for CNCs compared to 6 hr observed for AC).

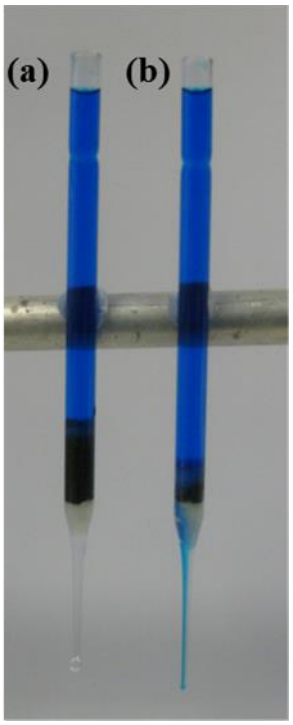

Figure 8. Image of set up to test the flowability of an aqueous media through sorbent materials (a) CNCs and (b) activated carbon.

Figure 8 shows the set up used to measure the flow of an aqueous media through a bed of carbon sorbents. The time taken for the aqueous media to transport through carbon materials was, on average, 282 and 580 s for CNCs and activated carbon, respectively. This is due to the larger pore volumes of CNCs as measured by N_2 physisorption (Figure 3) which are mainly mesoporous, compared to the AC which contains a mix of microporous and narrow mesoporous regions hindering the flow of aqueous media. The facile flow of an aqueous

media through the CNCs, when compared to ACs, is advantageous when selecting a carbon based material for fixed bed adsorbent applications.

3.2 CNCs as an Adsorbent of Pb Ions from Aqueous Solutions

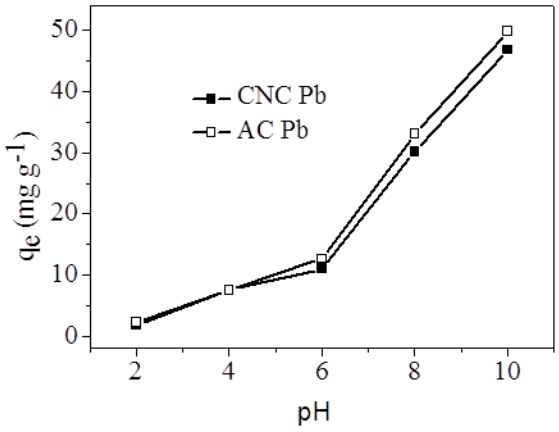

Figure 9. Graph showing the effect of pH on the uptake of Pb^{2+} ions by purified CNC and AC adsorbents. The concentration of Pb^{2+} ions was 25 mg dm^{-3}; (solution volume = 20 ml); sorbent loading was 10 mg; agitation time = 4 hr.

Figure 9 shows the adsorption of Pb^{2+} ions onto the surface of CNCs and AC as a function of solution pH. The increase in the adsorption of Pb^{2+} ions with increasing pH for both the CNC and AC samples suggests that an ion exchange mechanism between the H^+ ions and metal ions occurs at the oxygen-containing functional groups on the surface of both adsorbents. Below a pH of approximately 6, Pb^{2+} will exist as free ions in solution [37], making their interaction with the surface unhindered. At pH values above 6, Pb hydroxide complexes form, *e.g.* $Pb(OH)^+$, $[Pb(OH)_2]$ and $[Pb(OH)_3]$, which can precipitate from solution [37]. Additionally, there will be an unfavourable interaction of these Pb hydroxide complexes with the surface of both the carbon adsorbent materials investigated. A 25 mg dm^{-3} Pb^{2+} solution at pH 7 was filtered prior to testing with the carbon adsorbents to remove any precipitates; which reduced the level of Pb^{2+} ions in solution to 16.4 mg dm^{-3}.

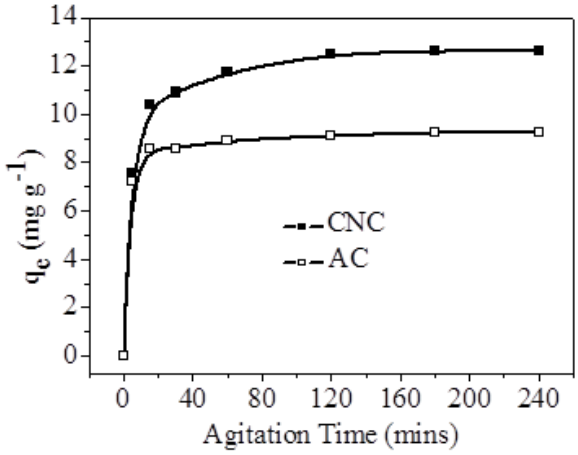

Figure 10. The uptake of Pb^{2+} ions onto the surface of purified CNCs and AC as a function of agitation time. The concentration of the Pb^{2+} ions used was 25 mg dm^{-3}; (solution volume = 20 ml); sorbent loading was 10 mg; pH 5 (50 mM acetate buffer).

Figure 10(a) shows the adsorption of Pb^{2+} ions onto the CNCs and activated carbon adsorbents as a function of agitation time. The initial Pb^{2+} solutions were buffered at pH 5 which ensured that the majority of Pb^{2+} ions remained as free ions in solution. The equilibrium adsorption of Pb^{2+} ions onto the surface of the CNCs and AC was achieved after 2 hr. The initial uptake of Pb^{2+} ions by the adsorbents was very fast for both materials, with over 80 % of the total uptake occurring within 15 minutes, and in accordance with other studies carried out on carbon-based sorption materials [38, 39]. Equilibrium adsorption reached 22.9 and 16.8 % of the total concentration of Pb^{2+} ions in solutions at pH 5 containing CNCs and AC respectively (which translates as q_e = 12.6 and 9.2 mg g^{-1}). The ion exchange mechanism on the surface of carbon adsorbents is supported by pH_{pzc} data obtained for both materials; below pH_{pzc} the surface will have an increasing net positive charge which in turn will create a repulsive interaction between the surface and positively charged heavy metal ions, hence decreasing uptake at lower pHs. The larger surface area, the greater number of oxidation sites and lower pH_{pzc} value of the CNCs makes them a more effective

adsorbent for Pb^{2+} ions at pH values below 6, compared to AC. The large pore volume of the CNCs (V_{tot} = 7.0 vs 0.3 cm^3 g^{-1}) also enhances the uptake of Pb^{2+} ions as previous studies undertaken with AC show that an increase in pore volume generally results in an increase in metal ion uptake due to facile diffusion [26].

Table 2. Pseudo-second-order kinetic data for the adsorption of Pb^{2+} ions on carbon adsorbents.

	Metal	k_2	R^2	h	$q_{e\ kin}$	$q_{e\ exp}$
		g mg^{-1} min^{-1}		mg g^{-1} min^{-1}	mg g^{-1}	mg g^{-1}
CNC	Pb	4.87×10^2	0.9995	8.038×10^4	12.853	12.592
AC	Pb	4.81×10^2	0.9999	4.069×10^4	9.200	9.230

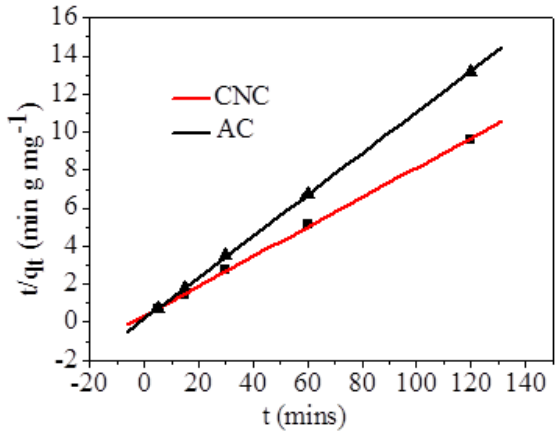

Figure 11. Pseudo second order plot of t/q_t vs t for Pb^{2+} ion adsorption showing linear fit of model to experimental data.

The adsorption of a solute onto a solid porous adsorbent can be broken up into three steps: (*i*) film diffusion of the solute to the sorbent surface at the solid (carbon sorbent) and liquid interface, (*ii*) intraparticle diffusion of the solute into the pores of the sorbent material and (*iii*) adsorption or binding of the solute to the external surface of the sorbent. The second-

order rate expression developed by Ho and McKay [40] can be applied to the adsorption of Pb^{2+} ions on carbon adsorbents and the rate coefficient of metal ion uptake can be derived from equation (2):

$$t/q_t = (1/k_2)q_e^2 + t/q_e \quad (2)$$

where q_t and q_e are the amounts of metal ion adsorbed (mg g^{-1}) on the carbon adsorbent at time (t) and at equilibrium time (e), respectively, t is agitation time (min) and k_2 is the second-order rate coefficient (g mg^{-1} min^{-1}) for the uptake of metal ions by carbon adsorbents. The product, $k_2q_e^2$ in the intercept term of the above equation expresses the initial sorption rate, h (mg g^{-1} min) as shown in equation (3):

$$h = k_2q_e^2 \quad (3)$$

The pseudo-second-order kinetic plots of t/q_t vs t are given in figure 11 for the two adsorbents. The second-order rate coefficient (k_2) and the equilibrium adsorption capacity (q_e) are calculated from the intercept and slope, respectively. These values together with the initial sorption rate (h) and regression coefficients are presented in table 2. The regression coefficients (R^2) for pseudo-second-order kinetic plots are above 0.999 for both carbon adsorbents interacting with Pb ions indicating that the kinetics of adsorption fits the pseudo second order model proposed by Ho and McKay. The model is further qualified by the comparison of q_e values from experimental results ($q_{e\ exp}$) and q_e values calculated from the kinetic plot ($q_{e\ kin}$) as the values correlate closely as shown in table 2. The rate coefficient (k_2) values calculated for the adsorption of Pb^{2+} ions shows no discernable difference between

the carbon adsorbents (table 2) whilst CNCs have a greater adsorption capacity which is derived from the kinetic plots $q_{e\ kin}$ of 12.85 mg g^{-1} for CNCs vs 9.2 mg g^{-1} for AC (table 2).

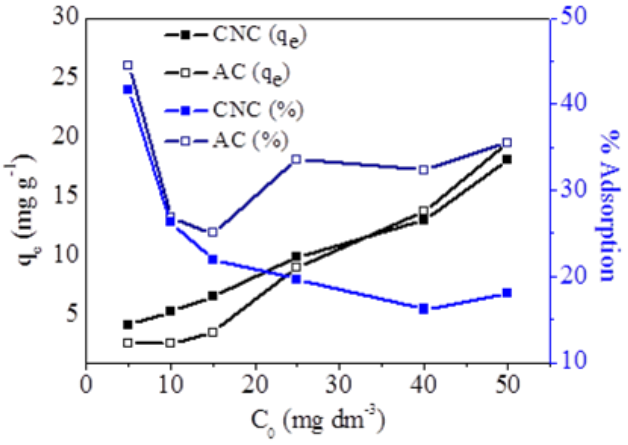

Figure 12. The uptake of Pb^{2+} ions onto the surface of purified CNCs and AC as a function of initial concentration (C_o) of metal ions. Agitation time = 4 h; solution volume = 20 ml; sorbent loading was 10 mg; pH 5 (50 mM acetate buffer).

Figure 12 shows the uptake of Pb^{2+} ions as a function of the initial concentration of metal ions where an upward trend of metal ion uptake (q_e) is recorded with increasing metal ion concentration. It is difficult to analyse where the materials reach saturation point but analysis of the uptake in terms of % adsorption indicates saturation point is reached at 40 mg dm^{-3} for CNCs.

4 Conclusions

High surface area CNCs have been successfully synthesised using a SCF deposition technique. The SCF process produces CNCs with surface areas of up to 1286 m^2 g^{-1}. The CNCs are highly dispersible for up to 24 h in an aqueous media and display excellent porosity which allows for the facile transport of an aqueous media through a fixed bed system when compared to activated carbon. The CNCs produced have an excellent adsorption

capacity for Pb^{2+} ions compared to commercially available AC, *i.e.* 11.1 and 7.6 mg g^{-1} respectively. The process by which Pb^{2+} ions are adsorbed onto CNCs and AC follows a pseudo second order model with similar rate coefficients (k_2) for both materials of approximately 4.8×10^2 g mg^{-1} min^{-1}. The adsorption process for both metal ions was largely pH dependent with both ions following very different patterns of metal ion uptake with increasing pH.

Acknowledgements

The authors would like to thank the EPA (Ireland) for financial support (Project: STRIVE 2007-PhD-ET-10).

5 References

[1] ATSDR, CERCLA Priority List of Hazardous Substances, (2007).

[2] The restriction of the use of certain hazardous substances in electrical and electronic equipment, O.J. L. 37 (2003) 19-23.

[3] S.A. Counter, L.H. Buchanan, F. Ortega, Neurophysiologic and neurocognitive case profiles of Andean patients with chronic environmental lead poisoning, J. Toxicol. Environ. Health Part A 72 (2009) 1150-9.

[4] S.K. Tandon, M. Chatterjee, a Bhargava, V. Shukla, V. Bihari, Lead poisoning in Indian silver refiners, Sci. Total Environ. 281 (2001) 177-82.

[5] D. Bagchi, S.J. Stohs, B.W. Downs, M. Bagchi, H.G. Preuss, Cytotoxicity and oxidative mechanisms of different forms of chromium, Toxicology 180 (2002) 5-22.

[6] J. Li, L. Li, H. Hou, Y. Fan, Study on the Reaction of polymeric zinc ferrocenyl carboxylate with Pb(II) or Cd(II), Cryst. Growth Des. 9 (2009) 4504-4513.

[7] A. Dabrowski, Z. Hubicki, P. Podkościelny, E. Robens, Selective removal of the heavy metal ions from waters and industrial wastewaters by ion-exchange method, Chemosphere 56 (2004) 91-106.

[8] G.A. Ottewill, G.W. Reade, S.A. Campbell, C.P. de Leon, F.C. Walsh, Electrochemical removal of metal ions from aqueous solution: a student workshop, J. Environ. Monit. 7 (2005) 943-9.

[9] T. Watanabe, H.-wei Jin, K.-jin Cho, Direct treatment of an acidic and high-strength nitrate-polluted wastewater containing heavy metals by using a bio-electrochemical reactor, Dev. Chem. Eng. Mineral Process. 13 (2005) 627-638.

[10] H. Bessbousse, T. Rhlalou, J. Verchere, L. Lebrun, Removal of heavy metal ions from aqueous solutions by filtration with a novel complexing membrane containing poly(ethyleneimine) in a poly(vinyl alcohol) matrix, J. Membr. Sci. 307 (2008) 249-259.

[11] N. Hamadi, Adsorption kinetics for the removal of chromium(VI) from aqueous solution by adsorbents derived from used tyres and sawdust, Chem. Eng. J. 84 (2001) 95-105.

[12] A. Sari, M. Tuzen, M. Soylak, Adsorption of Pb(II) and Cr(III) from aqueous solution on Celtek clay, J. Hazard. Mater. 144 (2007) 41-6.

[13] D.H. Lee, H. Moon, Adsorption equilibrium of heavy metals on natural zeolites, Korean J. Chem. Eng. 18 (2001) 247-256.

[14] B. Xiao, K.M. Thomas, Competitive adsorption of aqueous metal ions on an oxidized nanoporous activated carbon, Langmuir 20 (2004) 4566-78.

[15] F. Di Natale, a Lancia, a Molino, D. Musmarra, Removal of chromium ions from [corrected] aqueous solutions by adsorption on activated carbon and char, J. Hazard. Mater. 145 (2007) 381-90.

[16] W.E. Oliveira, A.S. Franca, L.S. Oliveira, S.D. Rocha, Untreated coffee husks as biosorbents for the removal of heavy metals from aqueous solutions., J. Hazard. Mater. 152 (2008) 1073-81.

[17] R. Gong, Y. Ding, H. Liu, Q. Chen, Z. Liu, Lead biosorption and desorption by intact and pretreated spirulina maxima biomass., Chemosphere 58 (2005) 125-30.

[18] M. Sekar, V. Sakthi, S. Rengaraj, Kinetics and equilibrium adsorption study of lead(II) onto activated carbon prepared from coconut shell, J. Colloid Interface Sci. 279 (2004) 307-13.

[19] X. Song, H. Liu, L. Cheng, Y. Qu, Surface modification of coconut-based activated carbon by liquid-phase oxidation and its effects on lead ion adsorption, Desalination 255 (2010) 78-83.

[20] M.A.A. Zaini, R. Okayama, M. Machida, Adsorption of aqueous metal ions on cattle-manure-compost based activated carbons, J. Hazard. Mater. 170 (2009) 1119-24.

[21] P. Patnukao, A. Kongsuwan, P. Pavasant, Batch studies of adsorption of copper and lead on activated carbon from Eucalyptus *camaldulensis dehn*. bark, J. Environ. Sci. 20 (2008) 1028-34.

[22] S. Babel, T.A. Kurniawan, Cr(VI) removal from synthetic wastewater using coconut shell charcoal and commercial activated carbon modified with oxidizing agents and/or chitosan, Chemosphere 54 (2004) 951-67.

[23] B. Girgis, Characteristics of activated carbon from peanut hulls in relation to conditions of preparation, Mater. Lett. 57 (2002) 164-172.

[24] N. Spahis, A. Addoun, H. Mahmoudi, N. Ghaffour, Purification of water by activated carbon prepared from olive stones, Desalination 222 (2008) 519-527.

[25] P.A. Bazuła, A.-H. Lu, J.-J. Nitz, F. Schüth, Surface and pore structure modification of ordered mesoporous carbons via a chemical oxidation approach, Microporous Mesoporous Mater. 108 (2008) 266-275.

[26] M. Nadeem, M. Shabbir, M.A. Abdullah, S.S. Shah, G. McKay, Sorption of cadmium from aqueous solution by surfactant-modified carbon adsorbents, Chem. Eng. J. 148 (2009) 365-370.

[27] J. Liu, L. Xu, W. Zhang, W.J. Lin, X. Chen, Z. Wang, Y. Qian, Formation of Carbon Nanotubes and Cubic and Spherical Nanocages, J. Phys. Chem. B. 108 (2004) 20090-20094.

[28] S. Ramesh, B. Brinson, M.P. Johnson, Z. Gu, R.K. Saini, P. Willis, T. Marriott, W.E. Billups, J.L. Margrave, Robert H. Hauge, R.E. Smalley, Identification of large fullerenes formed during the growth of single-walled carbon nanotubes in the HiPco process, J. Phys. Chem. B. 107 (2003) 1360-1365.

[29] C. Lu, H. Chiu, H. Bai, Comparisons of adsorbent cost for the removal of zinc (II) from aqueous solution by carbon nanotubes and activated carbon, J. Nanosci. Nanotechnol. 7 (2007) 1647-1652.

[30] K. Dasgupta, S. Kar, R. Venugopalan, R.C. Bindal, S. Prabhakar, P.K. Tewari, S. Bhattacharya, S.K. Gupta, D. Sathiyamoorthy, Self-standing geometry of aligned carbon nanotubes with high surface area, Mater. Lett. 62 (2008) 1989-1992.

[31] F. Li, Y. Wang, D. Wang, F. Wei, Characterization of single-wall carbon nanotubes by N_2 adsorption, Carbon. 42 (2004) 2375-2383.

[32] B.Y. Xia, J.N. Wang, X.X. Wang, J.J. Niu, Z.M. Sheng, M.R. Hu, Q.C. Yu, Synthesis and application of graphitic carbon with high surface area, Adv. Funct. Mater. 18 (2008) 1790-1798.

[33] Z. Li, M. Jaroniec, P. Papakonstantinou, J.M. Tobin, U. Vohrer, S. Kumar, G. Attard, J.D. Holmes, Supercritical fluid growth of porous carbon nanocages, Chem. Mater. 19 (2007) 3349-3354.

[34] K.S.W. Sing, D.H. Everett, R.A. Haul, L. Moscou, R.A. Pierotti, J. Rouquerol, T. Siemieniewska, Reporting physisorption data for gas/solid systems with special reference to the determination of surface area and porosity, Pure Appl. Chem. 57 (1985) 603-619.

[35] L. Ni, K. Kuroda, L. Zhou, T. Kizuka, K. Ohta, K. Matsuishi, J. Nakamura, Kinetic study of carbon nanotube synthesis over Mo/Co/MgO catalysts, Carbon. 44 (2006) 2265-2272.

[36] E.J. Bottani, E.A. Castro, Adsorption by Carbons, 1st ed., Elsevier, 2008.

[37] C. Faur-Brasquet, Z. Reddad, K. Kadirvelu, P.L. Cloirec, Modeling the adsorption of metal ions (Cu^{2+}, Ni^{2+}, Pb^{2+}) onto ACCs using surface complexation models, Appl. Surf. Sci. 196 (2003) 356-365.

[38] P. Shekinah, K. Kadirvelu, P. Kanmani, P. Senthilkumar, V. Subburam, Adsorption of lead(II) from aqueous solution by activated carbon prepared from *Eichhornia*, J. Chem. Technol. Biotechnol. 77 (2002) 458-464.

[39] Y. Li, Lead adsorption on carbon nanotubes, Chem. Phys. Lett. 357 (2002) 263-266.

[40] Y.S. Ho, G. McKay, Pseudo-second order model for sorption processes, Process Biochem. 34 (1999) 451-465.